Journal of Hydrology (N.Z.) Vol 24 No. 1, 1985

MODELLING THE CHRISTCHURCH AQUIFERS

Lee Kok Boon and Bruce Hunt

Department of Civil Engineering, University of Canterbury, Christchurch, New Zealand.

ABSTRACT

Currently available field data, mainly estimates for aquitard thicknesses and permeabilities, are used to construct two models of the layered aquifer system that exists beneath Christchurch, New Zealand. A finite-difference model is constructed and used to estimate piezometric head distributions that existed before abstractions began, and a semi-analytical model is constructed to estimate drawdowns in the neighbourhood of abstraction wells. Despite limitations in the accuracy and extent of present-day data, the semi-analytical model furnishes the most accurate method currently available for estimating the effect of future groundwater abstractions from the Christchurch aquifers.

INTRODUCTION

The North Canterbury Catchment Board currently gathers and interprets groundwater data for the major aquifers that lie beneath the city of Christchurch, New Zealand. These aquifers consist of at least five highly permeable sand and gravel layers separated by considerably less permeable layers of fine-grained sands, silts and peats. The explored portions of these aquifers extend downward to about 150 m below mean sea level and cover an area of approximately 300 km^2. These high-yielding aquifers are of major economic value to Christchurch since they are the source of all fresh water used within the city.

Although published data for the Christchurch aquifers has been accumulating for at least 75 years, the amount and quality of data needed for a major modelling effort is far from complete. Nevertheless, the writers were requested by the Catchment Board to construct a numerical model for two purposes: (1) to provide a management tool that can be used to estimate the effect of future water abstractions, and (2) to learn the amount and type of data that should be gathered in the future to improve the model.

AQUIFER DATA

A plan view of the area of the Canterbury Plains defined as the solution domain is shown in Figure 1. This region is bounded on the east by the seacoast, and on the west by the dividing line between the confined aquifer that extends beneath Christchurch and an unconfined aquifer that extends westward. The northern boundary coincides with a streamline drawn from measured piezometric contour maps, and the southern boundary with a similarly obtained streamline that skirts the northern edge of Banks Peninsula. The region roughly measures 18 km by 17 km and contains an area of about 300 km^2.

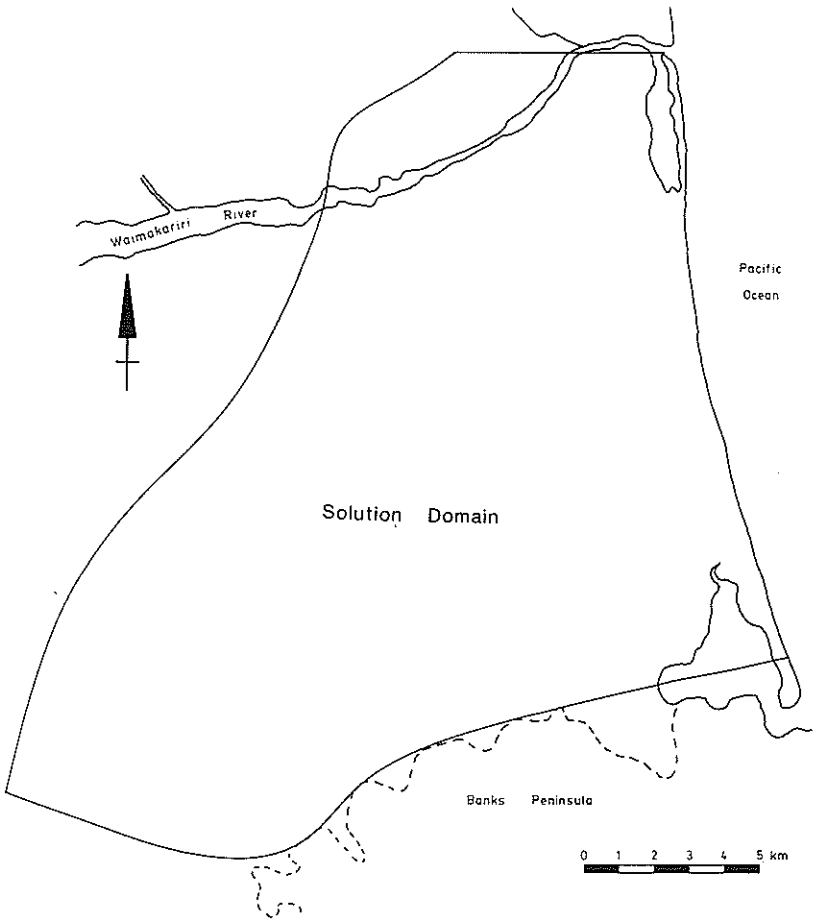

FIG.1 – A plan view of the area of the Canterbury Plains defined as solution domain.

Unpublished geologic cross sections drawn by J.H. Weeber from well logs suggest that the solution domain in Figure 1 is underlain by a series of five confined aquifers. The top boundary of the upper confined aquifer is believed to be relatively impermeable and is modelled herein as an aquiclude. All of the other confining layers, on the basis of pump tests and geologic data, are believed to be semi-permiable and are modelled as aquitards. Thus, leakage is assumed to occur in the vertical direction between different aquifers. Little is known about the fifth aquifer, which starts at about 150 m below mean sea level, since only a few of the deepest wells barely penetrate the top portion of this aquifer. A schematic cross section of the aquifers is shown in Figure 2.

If it is assumed that velocities within each aquifer are horizontal and that

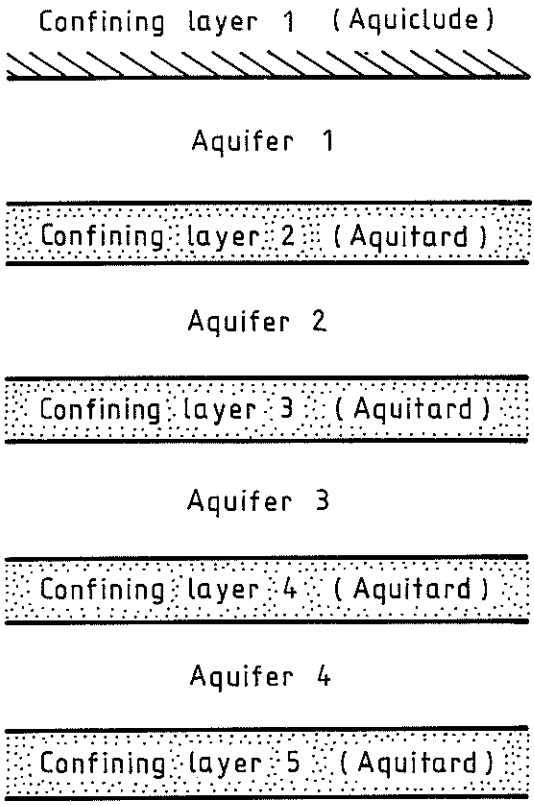

FIG.2—A schematic cross section of the solution domain.

leakage between aquifers occurs only in the vertical direction, then the movement of water in aquifer i is described by solutions of the equation

$$\frac{\partial}{\partial x}\left(T_i \frac{\partial h_i}{\partial x}\right) + \frac{\partial}{\partial y}\left(T_i \frac{\partial h_i}{\partial y}\right) = L_{i+1}(h_i - h_{i+1}) + L_i(h_i - h_{i-1}) + \frac{Q_i}{A} \qquad (1)$$

in which h_i=piezometric head in quifer i; T_i=transmissivity in aquifer i; L_i=leakance of aquitard i; Q_i=flow rate from a well in aquifer i; A=area surrounding the well and x and y=horizontal Cartesian coordinates. The function Q_i is zero everywhere except in the neighbourhood of the well, and, if $A \rightarrow 0$, then Q_i/A can be represented formally by using the Dirac delta function. The transmissivity, T_i, is the product of the aquifer thickness and coefficient of permeability, and the leakance, L_i, is the vertical aquitard permeability divided by the aquitard thickness. Thus, since confining layer 1 in Figure 2 is impermeable, $L_1=0$.

The solution of (1) for h_i can be obtained only after distributions of T_i and L_i have been calculated for each aquifer and aquitard, respectively. In this instance, values for these variables were computed from their definitions by using estimated thicknesses and permeabilities for the aquifers and aquitards. Contour maps showing aquifer and aquitard thicknesses were prepared by using unpublished geologic cross sections obtained by J.H. Weeber of the North Canterbury Catchment Board. Examples of these contour maps are shown in Figures 3 and 4. Contours are extrapolated in regions where well logs are currently unavailable, and the area of extrapolation increases as the depth to each layer increases. So little is known about the fourth aquifer and fifth confining layer that it was necessary to assume uniform thicknesses of 18 m and 12 m, respectively, for these layers. The contour maps made obvious the regions where most geologic information is needed.

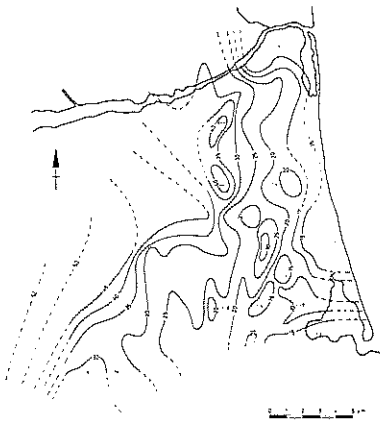

FIG.3—The thickness distribution for aquifer 1. Extrapolated contours are shown with dashed lines.

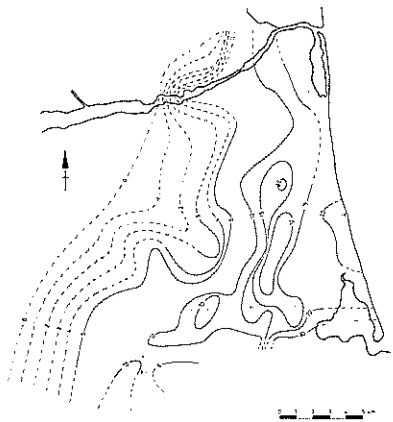

FIG.4—The thickness distribution for aquitard 2. Extrapolated contours are shown with dashed lines.

Permeability data for both aquifers and aquitards must be obtained from field pumping tests. Only one pumping test has so far been carried out within the solution domain, which suggests that more tests should be conducted in the future. This pumping test was carried out by Richards (1976) at Travis Swamp in eastern Christchurch and gave an aquitard permeability of 1.82×10^{-5} m/s. A representative aquifer permeability, which was obtained by averaging the Travis Swamp result with a result obtained from a second test just off the southwest boundary of the solution domain in Figure 1, was chosen as 3.94×10^{-3} m/s. Thus, aquitard permeabilities are about two orders of magnitude smaller than aquifer permeabilities, although neither are known with a great deal of certainty.

THE FINITE-DIFFERENCE MODEL

A finite-difference model was constructed using a finite-difference grid (Fig. 5). This grid, which is for aquifer 1, has a node spacing of 1 km and a

total of 325 nodes. The grid for aquifer 1 is used to generate the grid for aquifers 2, 3 and 4 by assuming that the solution domain is prismatic in the vertical direction. The entire three-dimensional grid has a total of 1300 nodes.

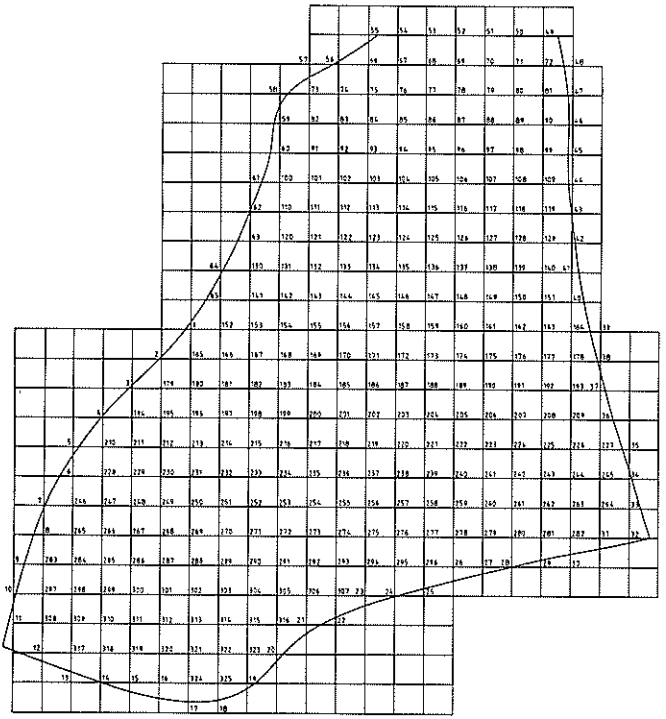

FIG.5—A finite-difference grid superimposed upon the solution domain.

Since the lateral boundaries of the solution domain are vertical surfaces, lateral boundary conditions for each of the top four aquifers are approximated using a method described by Hunt (1983) for two-dimensional problems. This method uses a first-order approximation for the equation.

$$\alpha \frac{dh}{dn} + \beta h = F \qquad (2)$$

in which n=arc length normal to the lateral boundary; F=specified function and α and β are specified functions that are usually chosen to be 0 and 1 or 1 and 0, respectively, along different segments of the solution domain boundary. The first-order algebraic approximation to (2) is used at all nodes that lie upon or adjacent to the lateral boundary in each aquifer. For this problem, values of (α, β, F) = (1, 0, 0) were used for all aquifers along the northern and southern boundaries (Fig. 1). Piezometric data given earlier

by Wilson (1976) suggests that piezometric heads have an insignificant change with depth along the western boundary. Thus, the model sets (α, β,) = (0, 1) and F equal to the same specified value along each vertical line for nodes that lie next to or upon the western boundary. Along the eastern boundary the model uses (α, β, F) = (1, 0, 0) for aquifers 2, 3 and 4 and (α, β, F) = (0, 1, 0) for aquifer 1. In other words, the eastern boundary is treated as impermeable for aquifers 2, 3 and 4 and as a reservoir boundary for aquifer 1. The set of boundary conditions along the eastern boundary was chosen because a salt water interface along the boundary can be approximated with this set of conditions. The piezometric data given by Wilson (1976) supports the use of these conditions and so little is known about this region that it would be difficult to assume any other set of conditions.

A second-order finite-difference approximation for (1) on the seven-node lattice (Fig. 6) can be obtained by integrating (1) throughout a rectangular area (Fig. 7). The result can be written in the form

$$\sum_{i=1}^{6} A_i h_i - A_0 h_0 = \frac{Q_0}{T_0} \tag{3}$$

in which

$$A_i = \frac{1}{2}\left\{1 + \frac{T_i}{T_0}\right\} \text{ for } i = 1, 2, 3 \text{ and } 4 \tag{4}$$

$$A_5 = \left\{\frac{\Delta}{l_{i+1}}\right\}^2, \quad (l_i \equiv \sqrt{T_0/L_i}) \tag{5}$$

$$A_6 = \left\{\frac{\Delta}{l_i}\right\}^2 \tag{6}$$

$$A_0 = \sum_{i=1}^{6} A_i \tag{7}$$

The grid spacing is Δ, $A_6 = 0$ for the top aquifer and h_5 is specified for the bottom aquifer.

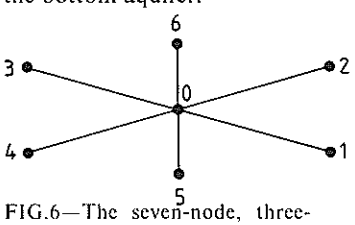

FIG.6—The seven-node, three-dimensional lattice used for the finite-difference representation of (1).

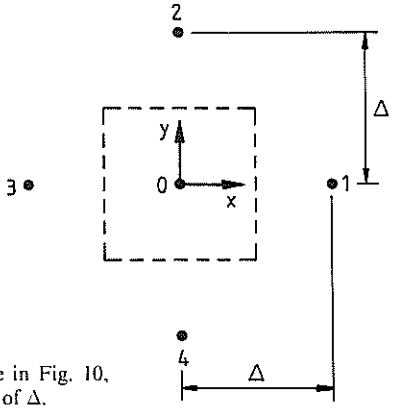

FIG.7—A plan view of the seven-node lattice in Fig. 10, which has a horizontal node spacing of Δ.

The set of linear algebraic equations given by (3) and the finite-difference approximations used for (2) were solved iteratively. The set of equations is diagonally dominant in the weak sense, which means that a solution by use of the Gauss-Seidel iteration is certain to converge (Varga, 1962). In practice, however, the convergence rate for the Gauss-Seidel iteration turned out to be so slow that it was abandoned. The reason for this lies in the relative magnitudes of the coefficients A_i in (3). Numerical values for A_i are about unity for i=1 through 4 and about seven for i=5 and 6. This means that an error in h_5 or h_6 takes a relatively long time to decay with the Gauss-Seidel iteration. The difficulty was solved by writing (3) in the form

$$A_5h_5 + A_6h_6 - A_0h_0 = \frac{Q_0}{T_0} - \sum_{i=1}^{4} A_ih_i \qquad (8)$$

Because A_0, A_5 and A_6 have large magnitudes relative to A_1, A_2, A_3 and A_4, errors in h_i on the right side of (8) lead to smaller errors for h_0, h_5 and h_6 on the left side. Furthermore, since nodes 0, 5 and 6 all lie along the same vertical line in the aquifer, and since A_6=0 for the top aquifer and h_5 is specified for the bottom aquifer, putting the newest estimates for h_i through h_4 on the right side of (8) gives a set of tridiagonal equations that can be solved efficiently by direct elimination for the next estimates of all unknown values of h that lie along the same vertical line. Repeating this calculation at all nodes until values of h ceased to change significantly gave an iterative solution technique that converged relatively rapidly.

A FINITE-DIFFERENCE APPLICATION

The finite-difference approximations just described approximate h within each aquifer by a third-degree polynomial and along all lateral boundaries by a first-degree polynomial. Since the radius of influence of almost any well

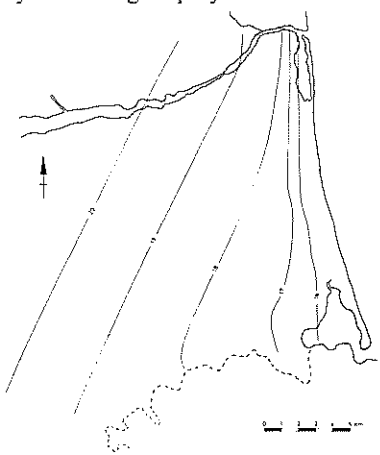

FIG.8—An estimate for the original piezometric head distribution in aquifer 1.

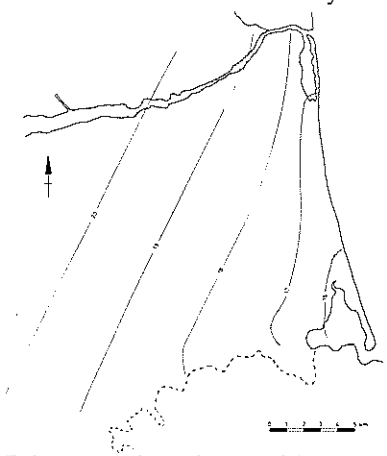

FIG.9—An estimate for the original piezometric head distribution in aquifer 3.

within the region is likely to be less than the node spacing of 1 km, the finite-difference model is not useful for predicting drawdowns created by a single well. In response to a request from the Catchment Board, however, this model was used to estimate piezometric head distributions that existed within each aquifer prior to the installation of wells within the solution domain. Some of these results are shown in Figures 8 and 9 and were obtained by using piezometric head measurements in the first wells penetrated aquifer 5 to estimate boundary values for the piezometric head on the bottom surface of aquitard 5. The solution is sensitive to large errors in this head distribution, which was necessarily obtained by using a minimum amount of field data. On the other hand, there is probably no way to improve estimates for these boundary values of h, which suggests that the accuracy of these results is unlikely to be improved upon.

THE SEMI-ANALYTICAL MODEL

Future model applications by the Catchment Board are most likely to be concerned with calculating drawdowns in the neighbourhood of abstraction wells. Since the finite-difference model is not useful for this purpose, it became necessary to consider a second model. One possibility would be to simply introduce more nodes into the finite-difference grid near each well. Because the finite-difference grid is actually three dimensional, this would introduce a great many more nodes into a grid that would have to be reformed for each application as well locations change. For this reason, it was decided to use a semi-analytical model whose accuracy is independent of the location and spacing of computational nodes.

The semi-analytical model is a solution of the following boundary-value problem:

$$\underline{T} \cdot \frac{1}{r} \frac{\partial}{\partial r} \left\{ r \frac{\partial \bar{h}}{\partial r} \right\} = \underline{L} \cdot \bar{h} \tag{9}$$

$$\text{Limit}_{r \to 0} \; \underline{T} \cdot \left\{ r \frac{\partial \bar{h}}{\partial r} \right\} = \frac{\bar{Q}}{2\pi} \tag{10}$$

$$\text{Limit}_{r \to \infty} \; \bar{h} = 0 \tag{11}$$

Vectors and matrices are denoted with overbars and underbars, respectively, in (9)-(11) and are defined as follows:

$$\bar{h} = \begin{bmatrix} h_1 \\ h_2 \\ h_3 \\ h_4 \end{bmatrix} \tag{12}$$

$$\bar{Q} = \begin{bmatrix} Q_1 \\ Q_2 \\ Q_3 \\ Q_4 \end{bmatrix} \tag{13}$$

$$\underline{T} = \begin{bmatrix} T_1 & 0 & 0 & 0 \\ 0 & T_2 & 0 & 0 \\ 0 & 0 & T_3 & 0 \\ 0 & 0 & 0 & T_4 \end{bmatrix} \tag{14}$$

$$\underline{L} = \begin{bmatrix} (L_1+L_2) & -L_2 & 0 & 0 \\ -L_2 & (L_2+L_3) & -L_3 & 0 \\ 0 & -L_3 & (L_3+L_4) & -L_4 \\ 0 & 0 & -L_4 & (L_4+L_5) \end{bmatrix} \tag{15}$$

The flow rate, Q_i, abstracted from aquifer i at the origin may be specified to be any number, including the number zero. Also, the leakance matrix, $\underline{L}$, has $L_1=0$ for this particular problem.

The transmissivity matrix, $\underline{T}$, and leakance matrix, $\underline{L}$, can both be shown to be symmetric and positive definite. Thus, Hildebrand (1965) shows that the following generalized eigenvalue problem always has four eigenvalues, λ_i, that are real and positive:

$$(\underline{L} - \lambda_i \underline{T}) \cdot \bar{U}_i = 0 \text{ for } i = 1, 2, 3 \text{ and } 4 \tag{16}$$

The eigenvectors, $\bar{U}_i$, are orthogonal relative to $\underline{T}$ and can be normalized to give

$$\bar{U}_i \cdot \underline{T} \cdot \bar{U}_j = \delta_{ij} \tag{17}$$

in which δ_{ij} = Kronecker delta. These results are used by Hunt (1984) to show that the solution of (9)-(11) is given by

$$\bar{h} = \frac{1}{2\pi} \sum_{i=1}^{4} (\bar{Q} \cdot \bar{U}_i) K_0 (r\sqrt{\lambda_i}) \bar{U}_i \tag{18}$$

in which K_0 denotes the zero-order modified Bessel function of the second kind. The asymptotic behavior of (18) for small r can be shown to be

$$\bar{h} \sim \frac{\bar{Q}_T}{2\pi} \ln(r) + \frac{1}{2\pi} \sum_{i=1}^{4} (\bar{Q} \cdot \bar{U}_i) [\ln (\sqrt{\lambda_i}/2) + \gamma] \bar{U}_i + \ldots . \tag{19}$$

in which γ = Euler's constant = 0.57721 . . . . and all omitted terms vanish as r→0. The vector Q_T in (19) is defined to be the vector that is obtained

by replacing Q_i with Q_i/T_i in (13). Thus, (19) shows that h_i remains finite as $r \to 0$ only in those aquifers for which $Q_i = 0$.

$\bar{h}$ may be evaluated from (18) at specified values of r, using the node where the well is located (Fig. 9), numerical values for the abstracted flow rates, Q_i, in each aquifer and values of r at which $\bar{h}$ is to be computed. The specified node and field data are used to construct the matrices $\underline{T}$ and $\underline{L}$, and a numerical solution of (16) is obtained by using a numerical algorithm. Finally, numerical values for $\bar{h}$ are calculated from (18) and (19) at the specified values of r.

A NUMERICAL EXAMPLE

A numerical example will be worked by assuming that an abstraction well is located in the third aquifer at node 158 (Fig. 5). The problem is to determine the maximum abstraction rate from this well if the drawdown created at a neighbouring well 500 m away in the same aquifer is to be less than 10 mm.

Since the flow rate to the well is not known, a solution is calculated by setting

$$\bar{Q} = \begin{bmatrix} 0 \\ 0 \\ 1 \\ 0 \end{bmatrix} \text{m}^3/\text{s} \qquad (20)$$

The solutions (Figs. 10-13), together with the results of using the finite-difference model, show the finite-difference solution becomes reasonably accurate only at horizontal distances greater than one node spacing from the

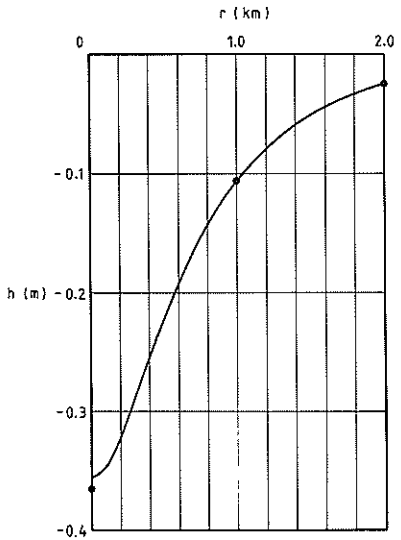

FIG.10—Drawdowns calculated in aquifer 1. Finite-difference results are shown with circles.

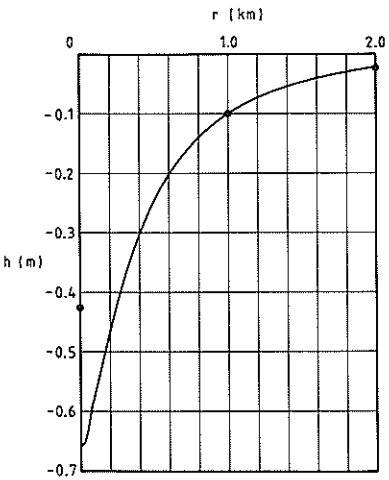

FIG.11—Drawdowns calculated in aquifer 2. Finite-difference results are shown with circles.

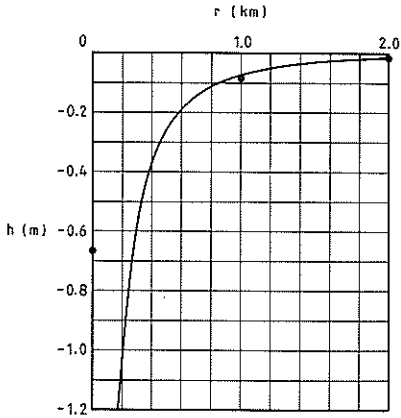

FIG.12—Drawdowns calculated in aquifer, 3 which is the pumped aquifer. Finite-difference results are shown with circles.

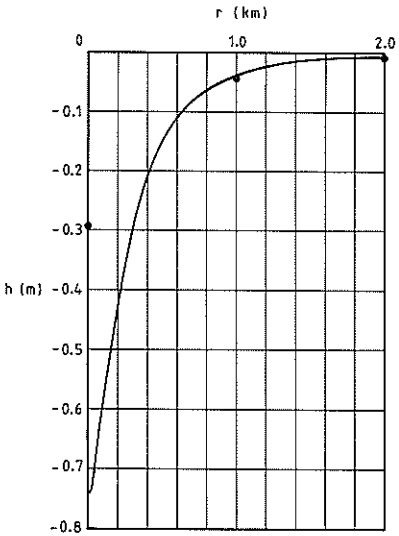

FIG.13—Drawdowns calculated in aquifer 4. Finite-difference results are shown with circles.

pumped well. At the pumped well itself the finite-difference model calculates a finite drawdown as the result of setting $A=\Delta^2$ in (1), and this, in turn, causes drawdowns above and below the well to be underestimated. Since the drawdown 500 m from the pumped well in aquifer 3 is 256 mm for a pumping rate of 1 m^3/s, and since the solution is directly proportional to this pumping rate, the pumping rate which will create a drawdown of 10 mm at r=500 m is

$$Q = \frac{10 \text{ mm}}{256 \text{ mm}} \times 1 \text{ m}^3/\text{s} = 0.039 \text{ m}^3/\text{s} \qquad (21)$$

Abstraction rates should not exceed the value given by (21) if drawdowns created at the neighbouring well are to not exceed 10 mm.

Lee (1985) shows how the semi-analytical model can be used, together with superposition and the method of images, to model the effects of lateral boundaries when the pumped well is located near a boundary of the solution domain. It should also be pointed out that superposition was used in writing (9)-(11) since heads at infinity and heads in the fifth aquifer for all values of r are assumed to vanish. Thus, solutions given by (18) and (19) differ only by a minus sign from drawdowns. The solution assumes that heads in aquifer 5 will not change, and this may not always be true for large flow rates abstracted from aquifer 4. This, of course, shows the need for finding out more about aquifers that lie below the top four aquifers.

CONCLUSIONS

Currently available data for aquifers beneath Christchurch have been

incorporated into the construction of two groundwater flow models. The finite-difference model is suitable for use in problems in which heads do not change rapidly over distances of the order of one kilometre. The semi-analytical model is suitable for modelling drawdowns created by a single well when the cone of depression for the well has a radius of less than about one kilometre. Both models show that future data collection should concentrate mainly upon determining aquifer and aquitard thicknesses and permeabilities. Efforts should also be made to explore the area that lies below the top four aquifers and to learn more about the aquifers and salt-water interface along the seacoast. Despite limitations in the accuracy and extent of present-day data, however, the semi-analytical model is the most accurate method currently available for estimating the effect of future abstractions from the Christchurch aquifers.

ACKNOWLEDGEMENTS

The writers would like to thank the North Canterbury Catchment Board and the Institution of Professional Engineers New Zealand for financial support. Help given by Messrs J.D. Talbot, J.H. Weeber and D.D. Wilson of the North Canterbury Catchment Board is also gratefully acknowledged.

REFERENCES

Hunt, B. 1983: *Mathematical Analysis of Groundwater Resources*, Butterworths, London, p. 54-57.

Hunt, B. 1984: Flow to a Well in a Multi-Aquifer System. To be published in the *Journal of Water Resources Research.*

Lee, K.B. 1985: Three-Dimensional, Steady-Flow Groundwater Models for the Christchurch Aquifers. Master of Engineering report, University of Canterbury, Christchurch, New Zealand.

Richards, G. 1976: Aquifer Test, Travis Swamp. Unpublished report to the North Canterbury Catchment Board.

Varga, R.S. 1962: *Matrix Iterative Analysis*, Prentice-Hall, Englewood Cliffs, p. 73.

Wilson, D.D. 1976: Hydrogeology of Metropolitan Christchurch. *Journal of Hydrology (N.Z.) 15 (2)*: 101-120.